Progress in Oceanography 218 (2023) 103117

Contents lists available at ScienceDirect

Progress in Oceanography

journal homepage: www.elsevier.com/locate/pocean

Responses of diatom assemblages and life cycle to sea ice variation in the eastern Indian sector of the Southern Ocean during austral summer 2018/2019

Kohei Matsuno [a,b,*], Kohei Sumiya [a], Manami Tozawa [a], Daiki Nomura [a,b,d], Hiroko Sasaki [c], Atsushi Yamaguchi [a,b], Hiroto Murase [e]

[a] Faculty/Graduate School of Fisheries Sciences, Hokkaido University, 3-1-1 Minato-cho, Hakodate, Hokkaido 041-8611, Japan
[b] Arctic Research Center, Hokkaido University, Kita-21 Nishi-11 Kita-ku, Sapporo 001-0021, Japan
[c] Fisheries Resources Institute, Japan Fisheries Research and Education Agency, 2-12-4 Fukuura, Kanazawa, Yokohama, Kanagawa 236-8648, Japan
[d] Field Science Center for Northern Biosphere, Hokkaido University, 3-1-1 Minato-cho, Hakodate, Hokkaido 041-8611, Japan
[e] Tokyo University of Marine Science and Technology, 4-5-7 Konan, Minato-ku, Tokyo 108-8477, Japan

ARTICLE INFO

Keywords:
Protist community
Cell size
Fragilariopsis
Indian sector of the Southern Ocean

ABSTRACT

In the Southern Ocean, rapid environmental changes (warming, freshening, and poleward shifts of the physiological fronts) are underway. These changes affect the distribution, abundance, and life cycle of protists. However, the spatial distribution of protists is not well understood in the eastern Indian sector of the Southern Ocean. We, therefore, evaluated the effects of environmental factors at the community level (abundance and species composition) and species-specific level (life cycle in diatoms) based on field sampling during the austral summer of 2018/2019. High chlorophyll levels and protist cell densities were observed in the eastern area from 120°E, in contrast to the distribution reported in the 1996 BROKE (The Baseline Research on Oceanography, Krill and the Environment) survey. This inter-annual variation was caused by differences in the sampling periods, nutrients, and zooplankton grazing pressures. North–south variation in protist abundance was well explained by silicate distribution, whereas sea ice variation did not influence it explicitly. The clustering of protist groups was well associated with nutrients, but locally, offshore groups were extended southward by currents and eddies. The cell size of the two dominant *Fragilariopsis curta* and *F. kerguelensis* exhibited similar significant relationships with sea ice variation and decreased 60 days after sea ice melted. Our findings demonstrate that sea ice changes do not clearly affect the protist community level but potentially affect the life cycle level of diatoms.

1. Introduction

In the Southern Ocean, the Antarctic Circumpolar Current (ACC) flows eastward offshore (between approximately 50°S and 65°S, Orsi et al., 1995), whereas the Antarctic Slope Current (ASC) flows westward along the coast of Antarctica. These circumpolar currents provide relatively constant environmental conditions. In recent years, warming and freshening trends and poleward shifts of the ACC fronts have been well described (Aoki et al., 2020; Hirano et al., 2021; Yamazaki et al., 2021). Accompanying the changes, a shallower mixed layer depth and intensified stratification occur (Sallée et al., 2010; Deppeler and Davidson, 2017), and these environmental changes could affect marine ecosystems (Moline et al., 2008; Deppeler and Davidson, 2017).

In the marine ecosystem of the Southern Ocean, phytoplankton forms a key component, and the most dominant taxon in phytoplankton is diatoms (Kopczynska et al., 1986). Diatoms bloom massively, accompanied by sea ice retreat during summer due to release from light limitation (Arrigo et al., 2010). Because the Southern Ocean is typical of high nutrient and low chlorophyll (HNLC) regions, iron from sea ice (containing a magnitude higher concentration of iron than typical Antarctic surface water) is believed to accelerate diatom growth (Martin et al., 1990; Lannuzel et al., 2016). Diatom assemblages can be altered by upwelling near the physical fronts (Chiba et al., 2000; Davidson et al., 2010).

Diatoms also play an essential role in the biological pump by exporting and cycling key nutrients (Ragueneau et al., 2006). Cell size in

* Corresponding author at: Faculty/Graduate School of Fisheries Sciences, Hokkaido University, 3-1-1 Minato-cho, Hakodate, Hokkaido 041-8611, Japan.
E-mail address: k.matsuno@fish.hokudai.ac.jp (K. Matsuno).

https://doi.org/10.1016/j.pocean.2023.103117

Available online 6 September 2023

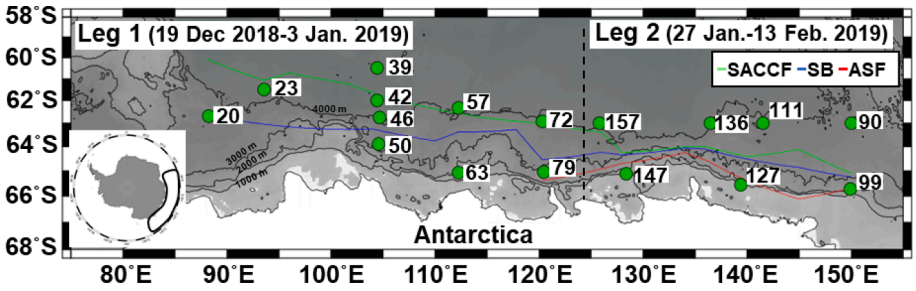

Fig. 1. Location of sampling stations in the Indian sector of the Southern Ocean during austral summer 2018/2019. SACCF: Southern Antarctic Circumpolar Current Front, SB: Southern Boundary of Antarctic Circumpolar Current, ASF: Antarctic Slope Front (Yamazaki et al., 2020).

diatoms is a critical factor that controls the sinking speed (Smetacek, 1985) and size-selective predation by zooplankton (Perissinotto, 1992). Owing to their functional roles, the diatom size structure considerably impacts the food web and material cycle in world oceans (Finkel et al., 2010; Marañón, 2015). Diatom size ranges from several micrometers to a maximum of 2 mm, with temporal changes in the life cycle (Edlund and Stoermer, 1997). Diatoms have two valves and propagate asexually through cell division. The parent valves divide, and each new daughter cell contains one parent valve and one new valve. Thus, the daughter cell becomes slightly smaller than the parent cell. With the progression of cell division, when the cell size reaches a critical lower limit, the sexual cycle is initiated, and auxospores are formed, increasing to the original larger cell size. Sea-ice dynamics can also influence the life cycle of diatoms through changes in nutrient availability, light climate, temperature, and stratification, which may affect phytoplankton bloom scale and size structure (Biggs et al., 2019). In the Southern Ocean, the dominant genus *Fragilariopsis* spp. is well-described for climate reconstruction and estimating sea-ice extent because its cell size relates strongly to environmental conditions (Cortese and Gersonde, 2007; Crosta, 2009). *F. kerguelensis* is a dominant species in diatom assemblages, and its size increases under high iron concentrations (Cortese and Gersonde, 2007). The size of *Fragilariopsis curta* is also known to increase with colder and wider sea ice extent (Crosta, 2009). Thus, diatom cell size is closely related to environmental changes and is an important factor affecting the material cycle and food web (Quetin and Ross, 1985; Jacques and Panouse, 1991; Kopczynska, 1992).

In the eastern Indian sector of the Southern Ocean (80–150°E), the BROKE (Baseline Research on Oceanography, Krill and the Environment, study period 1996) was an extensive campaign to investigate the standing stock of Antarctic krill (Nicol et al., 2000). In the campaign, diatom cell density and community structure varied with longitude, and the spatial–temporal variations could be explained by the sampling date, nutrients, trace metals, and zooplankton grazing (Waters et al., 2000). In addition, in the western Indian sector of the Southern Ocean (30–80°E), diatom assemblages change mainly through fronts and upwelling (Davidson et al., 2010). However, compared to several studies of diatom variation conducted in the Weddell Sea, Ross Sea, and Scotia Sea (e.g., Jacques and Fukuchi, 1994), knowledge of the eastern Indian sector of the Southern Ocean is limited. Considering the response by diatoms to environmental changes, only the distribution of *F. kerguelensis* can be predicted using species distribution modeling (Pinkernell and Beszteri, 2014). Because the environmental drivers restricting diatom assemblages and cell size are not well described, the effect of environmental changes (i.e., warming, freshening, upwelling) on diatoms in this region cannot be predicted.

In this study, we investigated the diatom cell density and community structure in the eastern Indian sector of the Southern Ocean during the austral summer of 2018/2019 to evaluate the relationship between diatoms and environmental factors. In addition, we measured the cell size of the dominant diatom species (*Fragilariopsis* spp.) and compared them with environmental parameters.

2. Material and methods

2.1. Field samplings

CTD (SBE-9plus, SBE-3plus, SBE-4C) casts were conducted at 17 stations in the eastern Indian sector of the Southern Ocean (60–65°S, 88–150°E) from 15th December 2018, to 23rd February 2019, on the R/V Kaiyo-Maru (2942 GT, Fisheries Agency of Japan) (Fig. 1). This study was conducted as a part of a multidisciplinary ecosystem survey in the eastern Indian sector of the Antarctic (CCAMLR [Commission for the Conservation of Antarctic Marine Living Resources] Division 58.4.1) with a focus on Antarctic krill. The survey was conducted over two Legs. Leg 1 was conducted from 19th December 2018 to 3rd January 2019 in the area from 88° to 120°E, and Leg 2 was conducted from 27th January to 13th February 2019, in the area from 125° to 150°E (Fig. 1, Supplementary Table 1). Vertical profiles of temperature, salinity, and fluorescence were measured using CTD casts. For enumeration and identification of diatoms, water samples (500 mL) were collected from the surface and an optical depth of 1 % photosynthetic available radiation (PAR) relative to the surface, was detected by a PAR sensor (Satlantic Inc., PAR-LOG ICSW), with a bucket and rosette of Niskin bottles (12 L) mounted on the CTD frame. After collection, samples were fixed and preserved in acid Lugol's solution (final concentration 1 %). For nutrient measurements, seawater samples (10 mL) were collected from the same depth for diatom cell count. The mixed layer depth was defined as the depth at which salinity was 0.05 greater than the value at 10 m depth (Clementson et al., 1998) (Supplementary Table 1). The Southern Antarctic Circumpolar Current Front (SACCF), Southern Boundary (SB) of ACC, and Antarctic Slope Front (ASF) were defined using the CTD and XCTD (Tsurumi Seiki Co., Ltd., MK-130) data (cf. Yamazaki et al., 2020).

2.2. Sample analysis

Post-voyage, the samples were concentrated 25- to 46-fold using siphon tubes (Sukhanova, 1978). Aliquots (0.3–1 mL) of the concentrated samples were transferred to a glass slide to count and identify the protists (diatoms, dinoflagellates, and ciliates) in approximately 300 cells using an inverted microscope (ECLIPSE Ts2R, Nikon) at 200–400× magnification with phase contrast. Only cells with cytoplasm and chloroplast were enumerated. Cells < 5 μm in size were not counted. The scanning electron microscope was not used for enumeration since this could have potentially induced an underestimation of <10 μm cells. Species identification was performed to the lowest possible level (species or genus) for the diatoms, as described by Hasle and Syvertsen (1997) and Pearce and Scott (2021). For ciliates, oligotrichs and tintinnids were counted. In addition, dinoflagellates and silicoflagellates were counted at the taxon level.

Additionally, the apical length of *Fragilariopsis curta* (2,974 cells) and *F. kerguelensis* (3,465 cells) was measured using an inverted microscope (ECLIPSE Ts2R, Nikon) and a software NIS-ELEMENTS D (Nikon) with an accuracy of 0.01 μm throughout the study region.

The concentrations of nitrate plus nitrite (NO_3^-+NO_2^-) and silicate (Si

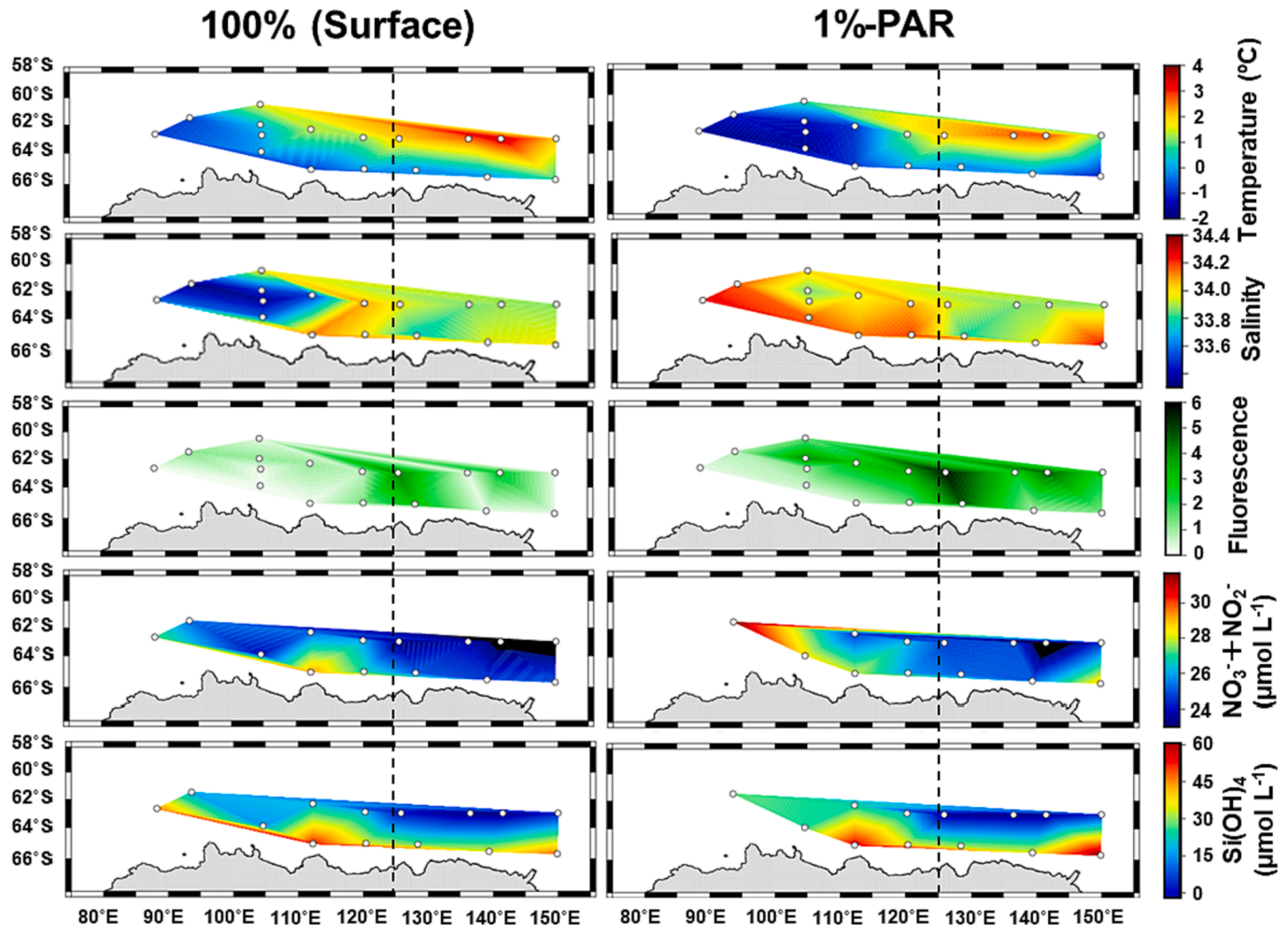

Fig. 2. Horizontal distribution of hydrography parameters at the surface (left panel) and 1 %-PAR (right panel) layers in the Indian sector of the Southern Ocean during the austral summer 2018/2019. Black dashed lines divide the areas of Leg 1 and Leg 2 (cf. Fig. 1).

$(OH)_4$) in the seawater were determined in accordance with the Joint Global Ocean Flux Study (JGOFS) spectrophotometric method (JGOFS, 1994) using auto-analyzer systems: a QuAAtro 2-HR system (BL-tec, Osaka, Japan) and a Seal Analytical System (Norderstadt, Germany). The analyzers were calibrated with reference materials for nutrient analysis (Lots BZ, CB, and CC; KANSO Technos Co., Ltd.). As accuracy index of the nutrients measurements, the standard deviations of the nutrient concentrations, calculated from 20 subsamples, for reference water samples (KANSO Technos Co., Ltd.), with NO_3^-+NO_2^- and $Si(OH)_4$ concentrations of 9.8 and 117.5 μmol L^{-1}, were 0.3 and 1.1 μmol L^{-1}, respectively.

2.3. Data analysis

To evaluate the sea ice melting date at each station, AMSR2 (Advanced Microwave Scanning Radiometer 2) and SSMIS (Special Sensor Microwave Imager/Sounder) data were obtained from the Arctic Data archive System (ADS, https://ads.nipr.ac.jp/). Time since sea-ice melt (TSM), defined as the period between the last day on which the sea ice concentration dropped below 15 % and the sampling date, was calculated using these data.

To reduce the bias for abundant species, the cell density data (X: cells L^{-1}) for each taxon/species were transformed to $\sqrt[4]{X}$ prior to cluster analysis (Quinn and Keough, 2002). The similarities between samples were examined using the Bray–Curtis index based on the differences in species composition. To group the samples, the similarity indices were coupled using hierarchical agglomerative clustering with a complete linkage method (an unweighted pair group method using the arithmetic mean: UPGMA) (Field et al., 1982). Similarity percentage (SIMPER) analysis was performed to determine which species contributed to the top 50 % of total abundance for each group. A species diversity index ($\acute{H}$) in each group was calculated using the equation:

$$\acute{H} = -\sum n/Ni \times \ln n/Ni$$

where n is the abundance (cells L^{-1}) of ith species, and Ni is the total protist abundance (cells L^{-1}) in the group (Shannon and Weaver, 1949).

The effects of different water zones (southern, subpolar, and continental zones) on the protist community were tested using permutational multivariate analysis of variance (PERMANOVA). A distance-based linear modeling (DistLM) and a distance-based redundancy analysis (dbRDA) were performed to reveal the relationship between environmental parameters and the protist community. To remove multicollinearity among the environmental parameters (mixed layer depth, PAR, temperature, salinity, fluorescence, nutrients (NO_3^-+NO_2^- and Si $(OH)_4$), and TSM), variance inflation factors (VIF) (Zuur et al., 2009) were calculated. Because all VIF values were below 5, none of the parameters were removed for the subsequent analysis. All environmental parameters were normalized, and DistLM was run with a dbRDA plot by combining the resemblance matrix (based on Bray–Curtis similarities between the abundances of protist species in the samples from both surface and 1 %-PAR layers) and the hydrographic variables. To run DistLM, selection procedures consisting of Step-wise, AICc (Akaike

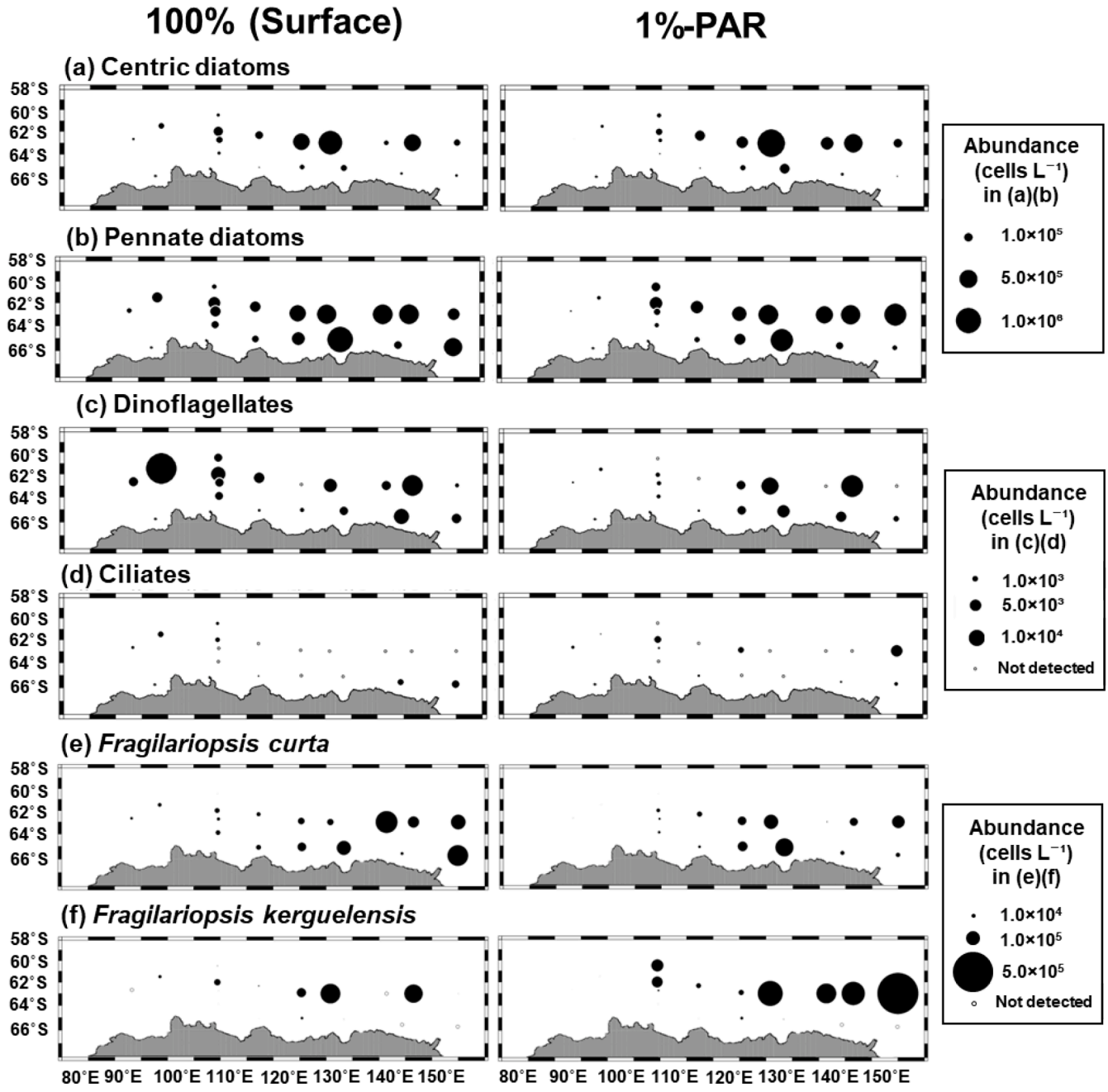

Fig. 3. Horizontal distribution of protist abundance in the Indian sector of the Southern Ocean during the austral summer 2018/2019.

information criterion corrected for small samples), and 999 permutations were used. Data were analyzed using Primer 7 software (PRIMER-E Ltd., Albany, Auckland, New Zealand). To identify potential indicator species in the groups that resulted from the cluster analysis, the program Indicator Value (IndVal) was used for each species (Dufrêne and Legendre, 1997).

Differences between sampling depths (surface vs. 1 % PAR layer) or among clustering groups on cell size of the dominant *Fragilariopsis* species were compared by Mann–Whitney *U* test and the max-t method with a heteroscedastic consistent covariance estimation (HC3) (Herberich et al., 2010). The tests were conducted using R software with the packages "multcomp" and "sandwich" (version 4.1.2, R Development Core Team, 2021). The relationship between the diatom size and environmental factors was analyzed using generalized additive modeling (GAMs) in R. The size data at all layers in all stations were combined for each species to run the GAMs.

The size structure of *Fragilariopsis* spp. was treated as a Tweedie distribution in the GAMs. A full model of GAMs with cell size as a response variable, and environmental parameters (temperature, nutrients (NO_3^-+NO_2^- and $Si(OH)_4$), and TSM) as explanatory variables was constructed (i.e., Size ~ s(Temperature) + s(nitrate + nitrite) + s(silicate) + s(TSM)). Since all stations (except three stations where CTD casts were conducted around mid-night) showed over 2 mol m^{-2} d^{-1} PAR (average 14.6 mol m^{-2} d^{-1}) at 1 % PAR layer, diatoms at the layer could produce at low level (Marañón et al., 2021). Due to that, we used the cell size data from the surface and 1 % PAR layers in GAMs. The environmental parameters were chosen because of suggested influences on diatoms cell size (cf. Cortese and Gersonde, 2007; Crosta, 2009) and avoidance to complicate the model. All statistical analyses were performed using R software with the package "mgcv" (version 4.1.2, R Core Team, 2021).

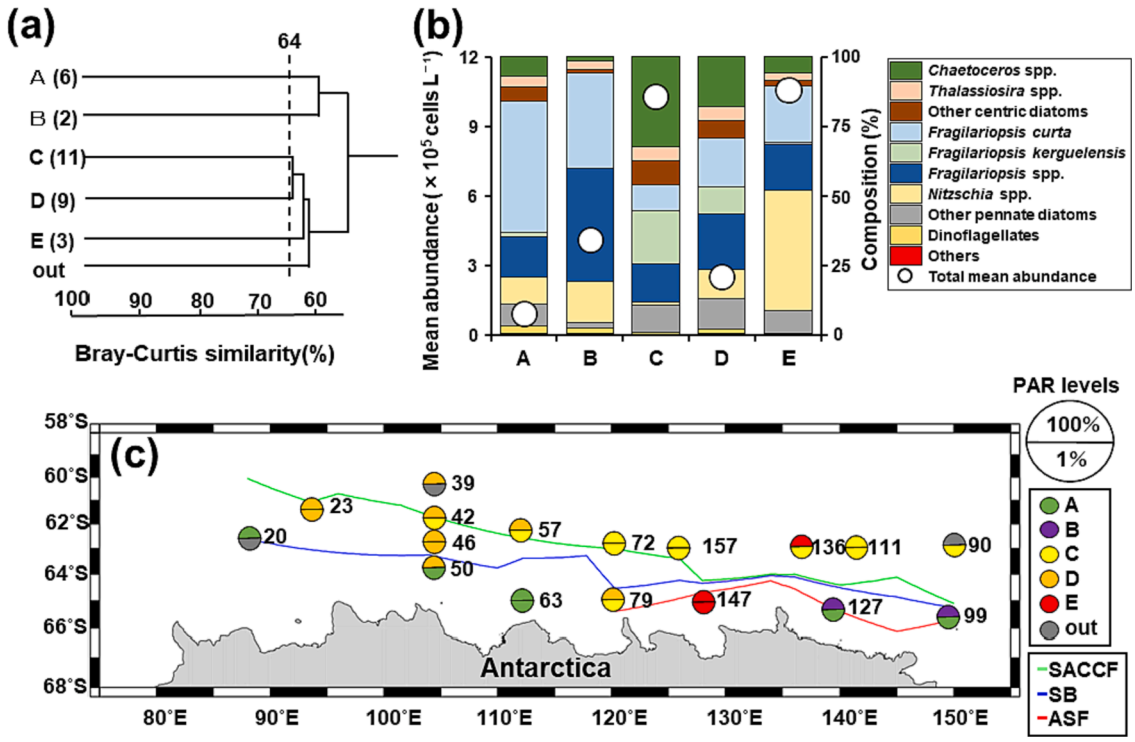

Fig. 4. Results of cluster analysis based on protist abundance by Bray–Curtis similarity connected with UPGMA. Five groups (A–E) were identified with the similarity at 64 % (dashed lines) (a). Numbers in parentheses indicate the number of stations included in each group. "Out" is defined that only one sample was included in the group. Mean abundance and species composition of each group (b). Geographic distributions of the five groups identified from Bray–Curtis similarity based on protist abundances in the Indian sector of the Southern Ocean during the austral summer 2018/2019 (c). SACCF: Southern Antarctic Circumpolar Current Front, SB: Southern Boundary of Antarctic Circumpolar Current, ASF: Antarctic Slope Front (Yamazaki et al., 2020).

3. Results

3.1. Hydrography

Except for St. 39, TSM ranged from 5 to 116 days and was higher in the northern area (Supplementary Table 1). The mixed layer depth was shallower in the northern area during Leg 1 (except at St. 39), whereas it was deeper in the southern area, particularly in Leg 2 (Supplementary Table 1). Temperature showed a similar spatial pattern in both layers, with cold water observed in the western and inshore areas (Fig. 2). Salinity, however, exhibited different spatial variations between the layers; fresh water was observed in the western area at the surface, but not at the 1 %-PAR layer. High fluorescence was observed in the eastern area in both layers, and the maximum (4.27–5.61) was observed at St. 157. Nutrients (NO_3^-+NO_2^- and $Si(OH)_4$) showed a clear latitudinal trend and were high in both layers in the inshore area.

3.2. Micro-protists

The abundance of the protists ranged from 8.7×10^4 to 1.7×10^6 and 1.8×10^4 to 2.1×10^6 cells L^{-1} at the surface and 1 %-PAR, respectively (Fig. 3). Diatoms were the dominant taxa in the study region (Fig. 3, Supplementary Table 2). In diatom distribution, the centric species were abundant in the offshore area, while pennate diatoms were dominant in the eastern area, especially St. 136 and 147 (Fig. 3). A total of 40 diatom species belonging to 21 different genera were identified (Supplementary Table 2). Dinoflagellate abundance was one order of magnitude lower than diatoms with a heterogeneous distribution. Ciliate abundance was low throughout the study period. *Fragilariopsis* spp. was the dominant genus, constituting 28–80 % of the protist assemblages. At the species level, *F. curta* was the most dominant species in ten samples, and *F. kerguelensis* was dominant in four samples. High abundances of them were observed offshore in the eastern area (Fig. 3).

Cluster analysis for abundance classified the protist assemblage into five groups (A–E) with 64 % similarity (Fig. 4a). Group A was observed in the southern area and characterized by the lowest abundance and dominance by *F. curta* (47 % in abundance) (Fig. 4). Group B occurred at the surface in the southeastern area (St. 99 and 127), and *Fragilariopsis* spp. (including all *Fragilariopsis* species) dominated up to 75 % of the group.

The largest group C was observed in the northern and eastern areas, with the highest number of species characterized by SIMPER (Table 1). *Chaetoceros* spp. and *F. kerguelensis* were 32 and 19 % in abundance, respectively. Group D was observed in the western area with a relatively low abundance. Group E, seen only at St. 136 and 147, exhibited the highest abundance with the dominance of 43 % in *Nitzschia* spp. (Fig. 4, Table 1). Relative high diversities were seen in groups C and D than in the other groups (Table 1).

The PERMANOVA analysis revealed that the water zone significantly did not influence the protist community composition (Supplementary Table 3). Each protist assemblage was roughly separated in the dbRDA plot (Fig. 5). Groups A and B were distributed in close locations, respectively, but groups C and D showed broader distributions (Fig. 5). As the best solution in DistLM, three environmental parameters were selected from eight parameters (i.e., mixed layer depth, PAR, temperature, salinity, fluorescence, nutrients (NO_3^-+NO_2^- and $Si(OH)_4$), and TSM), and these accounted for 38.7 % of the protist variation (Table 2). In the results, the two variables were categorized as nutrients (NO_3^-+NO_2^- and $Si(OH)_4$), and the remaining variable was fluorescence (Table 2).

3.3. Size structure in Fragilariopsis

Compared to the size between PAR levels, *F. curta* did not show significant differences (Table 3, Fig. 6). But in 18–21 μm, more *F. curta* were observed in the surface (506 cells) than in the deep layer (393

Table 1
Mean abundance of all taxa and diversity of microplankton in the Indian sector of the Southern Ocean during the austral summer 2018/2019. The five regions were identified from a cluster analysis of protist abundance using a Bray–Curtis similarity connected with UPGMA (cf. Fig. 4). Bold indicates IndVal of greater than 25 % for that group. *Represents top 50 % of species in each group according to SIMPER analysis. Number in () represents N, number of sampling stations.

Taxa	Abundance (cells L^{-1})				
	A (6)	B (2)	C (11)	D (9)	E (3)
Centric diatoms					
Asteromphalus hookeri	257	0	**3097**	504	728
Chaetoceros atlanticus	357	0	**68,637**	1478	1588
Chaetoceros bulbosus	0	0	**6738**	0	0
Chaetoceros castracanei	0	0	0	358	0
Chaetoceros concavicornis	585	0	**21,054**	2011	1720
Chaetoceros convolutus	925	**5323**	1927	833	3000
Chaetoceros curvisetus	285	0	6038	808	0
Chaetoceros dichaeta	583	265	**44,967**	3854	**18,858***
Chaetoceros neglectus	3048	794	20,393	**15,591***	8183
Chaetoceros peruvianus	103	0	**5274**	2007	0
Chaetoceros radicans	0	0	0	**5912**	0
Chaetoceros simplex	0	0	**5584**	827	2560
Chaetoceros spp.	562	0	**152,796***	11,891*	24,501
Corethron inerme	0	0	1122	**1023**	0
Corethron pennatum	730	2389	3381	1312	**5427**
Dactyliosolen antarcticus	227	0	**24,882**	1493	0
Guinardia cylindrus	347	0	**52,712***	7145*	2580
Leptocylindrus danicus	157	1066	868	1510	1280
Neomoelleria antarctica	0	0	1133	370	1280
Odontella weissflogii	183	0	494	482	**4035**
Proboscia alata	**1633**	0	0	406	860
Proboscia truncata	0	0	0	0	**1720**
Rhizosolenia spp.	1029	1323	621	1614	2008
Thalassiosira spp. < 20 μm	3089	11,184*	**39,151***	9316*	18,457
Thalassiosira spp. > 20 μm	862	1058	**11,439**	4212	**13,210**
Pennate diatoms					
Amphiprora belgicae	0	0	0	878	0
Banquisia belgicae	0	0	601	0	860
Fragilariopsis curta	44,630*	**142,516***	96,523*	44,340*	**215,164***
Fragilariopsis cylindrus	575	1604	661	1183	**17,117**
Fragilariopsis kerguelensis	1749	0	**196,894***	24,609*	5999
Fragilariopsis ritscheri	464	0	**16,556***	4813	**28,440**
Fragilariopsis separanda/rhombica	3433*	1852	**96,000***	21,513*	38,027*
Fragilariopsis spp.	9172*	**161,974***	27,059	23,195	**90,152***
Haslea trompii	909*	**2926**	**3763**	1936	1280
Membraneis challengeri	0	0	**982**	54	0
Navicula spp.	1083	2381	**10,948**	3798	**8867**
Nitzschia spp.	9153*	61,853*	12,512	27,364*	**459,484***
Plagiotropis gaussii	625	0	1844	583	**7299**
Pseudonitzschia spp.	4779*	2389	**80,524***	19,359*	**66,587***
Trichotoxon reinboldii	41	0	**2970**	824	0
Dinoflagellates	2371*	**7960***	6714	4053	5315
Tintinnid ciliates	0	**1066**	187	89	0
Oligotrich ciliates	496	**1595**	850	447	0
Silicoflagellates	201	0	1044	1050	**1588**
Total microplankton	94,641	411,517	1,028,942	255,045	1,058,172
Shannon–Weaver diversity	1.90	1.70	2.45	2.60	1.89

cells). There is also a bit larger *F. curta* in 26–28 μm (123 cells [100 %-PAR] vs. 92 cells [1 %-PAR]), which induces an insignificant difference in mean size between PAR levels. In contrast, smaller cells of *F. kerguelensis* were observed in the deeper layer (Table 3, Fig. 6). Intergroup comparison of the size for both species showed similar results, thus, larger cells were found in the southern stations (clustered in groups A and B) while smaller cells were seen in the northern stations (clustered in group C) (Table 3). As a result of the spatial variation in cell size for the species analyzed by GAMs, *F. curta* had significant relationships with temperature, $NO_3^-+NO_2^-$, $Si(OH)_4$ and TSM, and *F. kerguelensis* with silicate and TSM (Fig. 7). The relationships appeared to be similar for both species; the size showed the highest peak at 60 days in TSM, decreased until 90–100 days, and then recovered (increased) at 110 days. For each species, greater than 2 °C positively influent the size of *F. curta*. Silicates roughly negatively relate to the size of both species.

4. Discussion

4.1. Spatial variation of diatom blooms

In the eastern Indian sector of the Southern Ocean, the phytoplankton generally blooms from January to March, with a delay in timing in the southern area. Blooms at 64°S typically appear in January/February, while further south at 66°30′S, the blooms appear from February to March (Gomi et al., 2005). The highest abundance of diatoms was observed at St. 157 in mid-February (Fig. 3), in conformity with those observed by Gomi et al., 2005. However, the stations in the southern area exhibited low fluorescence with low cell density, even at high nutrient concentrations (Figs. 2 and 3). Generally, a deep mixed layer prevents phytoplankton from maintaining a suitable depth for active growth (Tilzer and Dubinsky, 1987; Samyshev, 1991). From another viewpoint, deep phytoplankton assemblages represent vertical flux in the biogeochemistry cycle with very little production (Lafond et al., 2020). As deeper mixed layer depths (48–63 m) were observed at

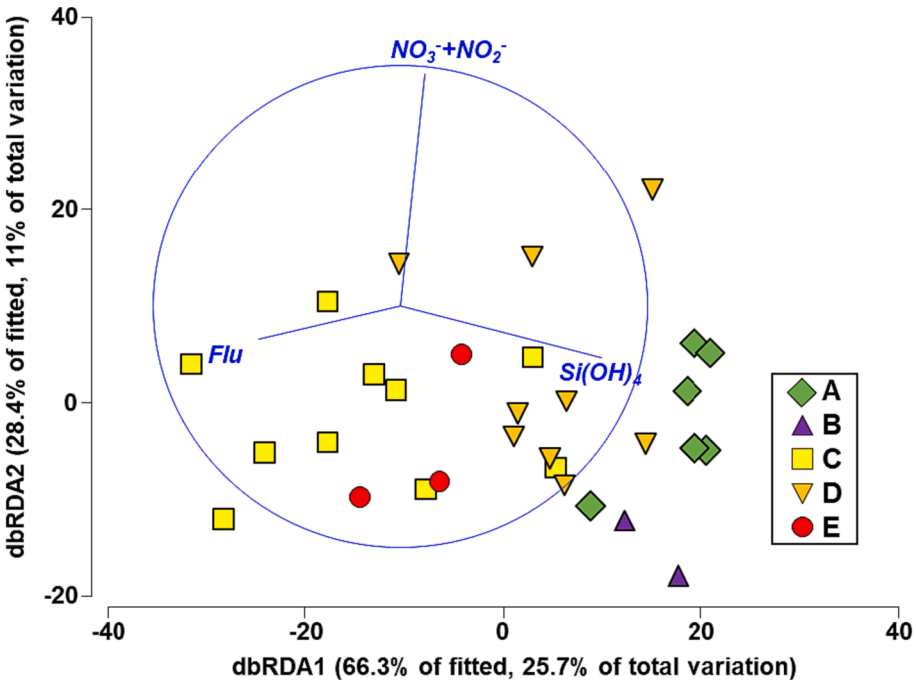

Fig. 5. dbRDA plot of the five groups with environmental parameters. The parameters were selected by procedures consisting of Step-wise, AICc (Akaike information criterion corrected for small samples) and 999 permutations were used. The direction and length of the lines indicate the relationship between groups and the strength of the relationship. Flu: fluorescence, NO_3^-+NO_2^-: nitrate + nitrite, and $Si(OH)_4$: silicate.

Table 2
Summary of the DistLM sequential tests. Selection procedures consisting of Step-wise, AICc (Akaike information criterion corrected for small samples) and 999 permutations were used. Results of the model with the lowest AICc values for each response variable. SS: sum of squares, Prop.: proportion of variance explained by each predictor variable, Cumul.: cumulative proportion of variance explained by each predictor variable, Res.df: residual degrees of freedom.

Variables	AICc	SS	Pseudo-F	*P* values	Prop.	Cumul.	Res.df
$Si(OH)_4$	227.78	5556.3	7.3274	0.001	0.18632	0.18632	32
NO_3^-+NO_2^-	225.31	3249.7	4.7937	0.001	0.10897	0.29529	31
Fluorescence	223.11	2754.1	4.5246	0.001	0.092354	0.387644	30

Table 3
Comparison of cell size of *Fragilariopsis* species between PAR level (surface vs. 1 % PAR) or among groups in the Indian sector of the Southern Ocean during the austral summer 2018/2019.

Species	Comparison between layers					Comparison among groups									
	Mean cell size (μm)		*U* test			Groups					Max-*t* test				
	Surface	1 %-PAR	*df*	*t* value	*p* value	A	B	C	D	E					
F. curta	21.3 ± 6.7	21.4 ± 6.9	2972	−0.47	0.6384	22.8 ± 7.1	22.6 ± 6.4	19.3 ± 5.5	21.1 ± 6.4	24.0 ± 7.7	C^3	D^2	B^1	A^1	E^1
F. kerguelensis	32.5 ± 12.0	30.7 ± 9.7	3463	−4.937	0.0001	37.3 ± 14.4	51.8 ± 18.3	29.6 ± 9.8	32.7 ± 10.7	30.3 ± 10.0	C^3	E^2	D^2	A^1	B^1

these stations (e.g., St. 63, 127) compared to those (14–30 m) in offshore stations (Supplementary Table 1), phytoplankton growth was limited by deep mixing. If the mixed layer becomes shallower, phytoplanktons bloom will potentially occur in the southern area, whereas offshore assemblages are under phytoplanktons bloom in the eastern area from 120°E due to fluorescence distribution (Tozawa et al., 2022).

During the 2018/2019 cruise, high cell abundances were observed in the area east of 120°E (Fig. 3). A previous study, however, indicated the opposite pattern of the east–west variation on analysis of diatom-Chl *a* by high-performance liquid chromatography and CHEMTAX (a program for estimating class abundances from chemical markers) (Wright and van den Enden, 2000). It was higher in the western area (90–120°E) in 1996 under the BROKE project (Wright and van den Enden, 2000). This inter-annual difference in the spatial distribution of diatoms could be explained by sampling date, environmental conditions, and zooplankton grazing impact. Basically, in the early period of the phytoplankton growing season (spring to autumn), the phytoplankton community quickly changes in a few weeks due to high growth rates with rapid species succession (Quéguiner, 2013). Regarding the sampling date, this study was conducted approximately one month earlier than that of the BROKE cruise (from 29th January to 21st March). The 1-month difference might have affected the spatial difference in diatoms due to the rapid shrinking of sea ice from November until mid-February in the Southern Ocean.

Comparing the hydrography between the western (88–120 °E) and eastern (125–150°E) areas in 2018/2019, the western area had lower salinity and shallower mixed layer depth at the surface layer (Fig. 2, Supplementary Table 1), suggesting that sea-ice meltwater made a

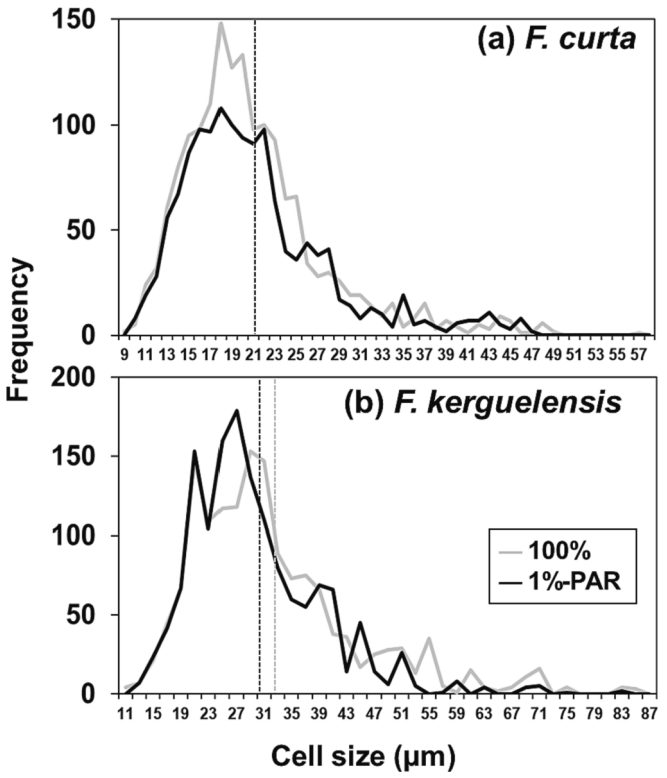

Fig. 6. Size frequency of *Fragilariopsis* species in the Indian sector of the Southern Ocean during austral summer 2018/2019. Size frequency was summarized every 1 μm bin for each layer. Solid grey and black lines represent the different sampling layers. Dashed grey and black lines are mean cell size for each layer (cf. Table 3).

shallower mixed layer. Because sea ice contains low levels of macronutrients (Clarke and Ackley, 1984; Dieckmann et al., 1991), diatoms could be trapped in the low-nutrient ice melted water at the surface, which would have restricted their growth. This was reflected in the difference in the protist assemblages; low-abundance group D occurred locally at the surface layer in the western area (Fig. 4). Comparison of the hydrographic features between groups C and D in dbRDA showed that group C was found at areas with low silicate (mean 37.35 μmol/L) and high fluorescence (mean 3.21) areas; conversely, group D was seen at areas with relatively high silicate (mean 44.82 μmol/L) and low fluorescence (mean 0.80) (Fig. 5). Therefore, since diatom assemblages could increase with the consumption of rich nutrients during the study period, high fluorescence and low nutrients in the eastern area were observed as a result of diatom bloom. Reflecting the active biological production in our study, higher pCO_2 and lower macronutrients were reported compared to the BROKE survey in 1996 (Tozawa et al., 2022).

As a potential consumer of diatoms, pteropods were abundant in the macrozooplankton community in the western area on the same cruise (Urabe et al., under review). Since pteropods can efficiently feed on small particles, including phytoplankton (Gilmer, 1972), protist assemblages may have been feeding on them, resulting in a low cell density occurring at group D stations in the western side of the sampling area (Fig. 4). The salps, yet another important filter feeder to diatoms, showed significant inter-annual changes between 1996 and 2018/2019 (Urabe et al., under review). Salp blooms observed in the eastern area in 1996 (Hosie et al., 2000) affected phytoplankton assemblages by feeding, resulting in low phytoplankton cell density. In contrast, almost no salp species were observed in 2018/2019 (Urabe et al., under review). Thus, in the eastern area, phytoplankton assemblages were not under grazing pressure by salps in 2018/2019, resulting in high diatom bloom.

4.2. Relationship between diatom assemblages and hydrography

Throughout the study region, low abundances were observed in groups A and B in the southern area, but high abundances were seen in groups C and E (except group D) in the offshore area (Fig. 4). It seems related to fronts, but no significant relation was detected in our study (Supplementary Table 3). On the other hand, the north–south difference in diatom assemblages might be caused by the mixed layer depth (as stated above), sea ice extent, and nutrients. Among the nutrients, silicate was selected as the significant parameter in dbRDA and not TSM (Fig. 5).

In general, sea ice melting controls the onset of phytoplankton blooms in the Southern Ocean (El-Sayed and Taguchi, 1981). After sea ice melts, the supply of iron from the ice stimulates phytoplankton growth (Sedwick and DiTullio, 1997), even in diluting the macronutrients (Kanna et al., 2014), resulting in its blooming in the stratified surface layer (El-Sayed and Taguchi, 1981; Marra and Boardman, 1984; Smith and Nelson, 1985; Fryxell and Kendrick, 1988). Based on iron-fertilized experiments in the Southern Ocean, iron mediate increases in phytoplankton growth, chlorophyll *a*, and primary production (Boyd and Law, 2001). From the viewpoint of seasonality, the phytoplankton bloom shifted from north to south in association with the time of melting of sea ice (Sokolov and Rintoul, 2009; Iida and Odate, 2014). In blooms, the nano-sized haptophyte *Phaeocystis antarctica* was predominant by forming colonial blooms in the marginal sea ice zone and ice edge (e.g., Davidson et al., 2010). As we did not analyze the nanoflagellates (i.e., *P. antarctica*), the contributions were unclear in this study. In contrast, ice-associated diatoms (*Amphiprora* spp., *Neomoelleria antarctica*, and *Odontella weissflogii*, cf. Gomi et al., 2005) were not abundant in groups A and B (Table 1). A similar group was observed at approximately 63°S from 17th February to 13th March 2000, and the community is weakly related to the ice edge (Gomi et al., 2005). Thus, diatom assemblages are strongly related to nutrient distribution during summer but weakly associated with sea ice variation.

In the offshore region, group D was observed in the western area, whereas group C was widely distributed in the eastern area (Fig. 4). Group D was characterized by low abundances and dominance of *Chaetoceros* spp. and *Fragilariopsis* spp. (including *F. curta* and *F. kerguelensis*), and was considered to be an intermediate community between groups A and C (Table 1). As mentioned above, the group may have been induced by sea ice meltwater on the surface. In contrast, group C was characterized by the dominance of *Chaetoceros* spp. and *F. kerguelensis* (Table 1). A similar observation on *Chaetoceros dichaeta* and *Chaetoceros neglectus* as dominant species in the Indian sector of the Southern Ocean is also on record (Gomi et al., 2005; Davidson et al., 2010). A planktonic diatom (*F. kerguelensis*) is also known to be abundantly present in the offshore region of the Southern Ocean (Iida and Odate, 2014) and around the polar frontal region (47–50°S) in the Atlantic sector during austral spring (de Baar et al., 1997). Since a similar diatom assemblage occurred as an offshore group in ACC in the western Indian sector (30–80°E) between January and March 2006 (Davidson et al., 2010), group C was considered a typical offshore community in the Southern Ocean.

Although spatial resolution in sampling stations was uneven in this study, a north–south difference of diatom assemblages was observed (Fig. 4c). Exceptions were high-abundance groups C and E found at St. 79 and 147 in the southern area (Fig. 4). This unique phenomenon is related to the surface current and upwelling (Wright and van den Enden, 2000). These stations are located in the shelf-break region (Fig. 1), where the bottom depth varies from 500 to 1500 m. A narrow westward slope current runs on the surface north of the shelf break, forming gyres that close at 115–120°E, indicating the presence of the southward current (Nicol et al., 2000). Additionally, multi-cyclone eddies transport heat poleward along the shelf break, based on the 2018/2019 reports of the same cruise and satellite observations (Hirano et al., 2021). Therefore, group C was potentially extended to the southern area by a continuous southward current and/or eddy (Nicol et al., 2000; Hirano

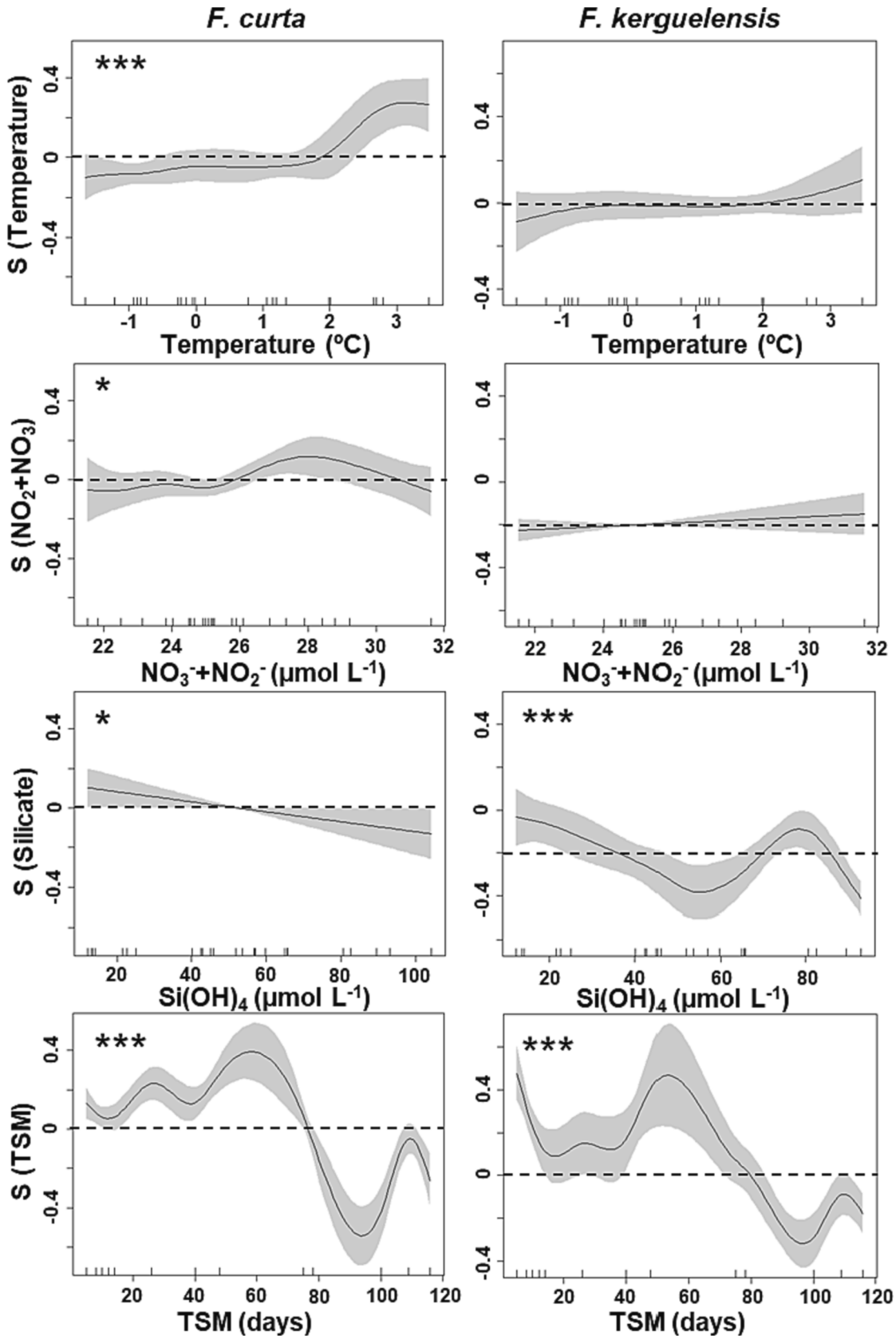

Fig. 7. Results of GAMs based on the size of two *Fragilariopsis* species with environmental parameters. Dashed lines indicate no effect. TSM: time since melt. *: $p < 0.05$, ***: $p < 0.001$.

et al., 2021), supporting the same diatom community. Additionally, upwelling frequently occurs when the slope current hits the slope and phytoplankton blooms are stimulated, resulting in high chlorophyll *a* levels (Strutton et al., 2000; Wright and van den Enden, 2000). Thus, the high-abundance group E was represented by the supply of rich nutrients by upwelling.

4.3. Size variation of Fragilariopsis spp. related with hydrography

Fragilariopsis spp. is dominant in phytoplankton assemblages in the Southern Ocean (Samyshev, 1991). The genus *F. curta* is an ice-algae species (Lizotte, 2001) and is dominant in the marginal ice zone and under/in the sea ice in the Southern Ocean (Garrison et al., 1987; Garrison and Buck, 1989; Kang and Fryxell, 1993; Hegseth and von Quillfeldt, 2002, Armand et al., 2005). The abundance and cell size of the species increase in colder and wider sea ice extent years (Crosta, 2009). In GAMs, significant relationships in cell size variation were detected with temperature (Fig. 7), but the relationship followed an opposite pattern compared to the previous report, caused by different timescales (several thousand years in Crosta, 2009 vs. one season in this study). Cell size exhibited significant relationships with nutrients, but the effect was not greater than that of temperature and TSM (Fig. 7). In contrast, TSM showed a relationship with the species' life cycle. In general, diatom cell size decreased until the sexual stage with cell divisions; after the formation of auxospores via sexual reproduction, diatoms eventually recovered their size. This indicated that *F. curta* continued cell division from 60 to 90 days in TSM and then recovered its cell size after 90 days in TSM. Additionally, based on the inter-group comparison, the cell size was significantly smaller in group C than in the other groups (Table 3); this means the *F. curta* actively grew in the group under the bloom.

Fragilariopsis kerguelensis is an important species contributing to the "opal belt" in the Southern Ocean (Zielinski and Gersonde, 1997; Cortese and Gersonde, 2007). According to Lafond et al. (2021), since *F. kerguelensis* below the mixed layer is mostly detrital (empty, broken or crunched), this species significantly contributes to vertical flux in biogenetic silica in the Southern Ocean. As vertical variation in the species, higher abundance was seen offshore in the eastern area at 1 % PAR layer with smaller cells (Fig. 3, Table 3). We did not count the detrital cells, but the result represents a remnant stock with very little *in situ* production. As this species has been dominant in diatom assemblages over the long term and frequently dominates in sediment, it has been well-studied as a biological indicator in paleobiology (Cortese and Gersonde, 2007; Crosta, 2009; Shukla et al., 2013; Kloster et al., 2018). Responding to environmental factors, *F. kerguelensis* exhibits an opposite pattern to *F. curta*; thus, their abundance increases in warm and lower sea-ice years (Crosta, 2009). This species' abundance and cell size are suggested to be increased by iron from sea ice (Cortese and Gersonde, 2007). In incubation experiments, higher iron concentrations produced larger cell sizes and higher growth rates (Timmermans and van der Wagt, 2010). Additionally, high iron concentrations stimulate the formation of auxospores, as revealed by field iron fertilization experiments (Assmy et al., 2006). Unfortunately, we did not measure iron concentration in this study, but hypothesized that the area in the lower TSM has detectable effects (i.e., larger cell size in the lower TSM) by iron supply from sea ice melt. As shown in the GAMs, a positive effect of TSM on cell size was observed in the lower TSM (Fig. 7), which suggests that iron supply from the sea ice melt stimulates the formation of larger cells and sexual reproduction process in *F. kerguelensis* as well as *F. curta*. Interestingly, the relationships between size and TSM were similar in *F. curta* and *F. kerguelensis* (Fig. 7), suggesting that *F. kerguelensis* possibly recovered their cell size by forming auxospores after 100 days in TSM.

In conclusion, the two dominant *Fragilariopsis* species had a significant relationship with TSM, although their biological features differed in geographical distributions and suitable temperatures. This indicates that these species grow actively after the sea ice melts and recover their size by making auxospores almost simultaneously. Thus, sea ice variations (e.g., sea ice extent and timing of melt) are pivotal factors that affect their life cycle. The smaller cell size also indicated a phytoplankton bloom region. But this study did not measure temporal variation in size directly. For future work, the temporal variation of cell size and growth rate of these species should be investigated under controlled conditions in the laboratory. It will improve our understanding of the response of protist assemblages to climate change in the Southern Ocean.

5. Conclusion

This study describes the spatial variation in protist assemblages in the eastern Indian sector of the Southern Ocean during the austral summer of 2018/2019. High chlorophyll *a* and cell density were observed in the eastern area from 120°E, which differs from the pattern reported in 1996. This inter-annual change was excluded by inter-annual differences in the sampling periods, nutrients, and zooplankton grazing pressure. North–south variation in protist abundance was explained by the presence of silicate, whereas sea ice variation did not influence it explicitly. Clustering groups were also well related to nutrients; however, locally, offshore groups were extended by southward currents and poleward eddies. The size variations in the two dominant *Fragilariopsis* species were significantly affected by the number of days after the melting of sea ice. In the eastern Indian sector of the Southern Ocean, sea ice changes do not affect the protist community level but affect the life cycle level of diatoms during summer. The findings will help the selection of critical environmental parameters for predicting diatom distribution, species composition, and size under climate change. Future studies should focus on the nutrients (including iron) cycle rather than sea ice variation to monitor phytoplankton assemblages.

Declaration of Competing Interest

The authors declare that they have no known competing financial interests or personal relationships that could have appeared to influence the work reported in this paper.

Data availability

Data will be made available on request.

Acknowledgments

We are deeply grateful to the officers, crew, and researchers onboard R/V Kaiyo-Maru for their assistance with biological sampling. The Kaiyo-Maru survey was supported by the Institute of Cetacean Research, the Japan Fisheries Research and Education Agency, and the Fisheries Agency of Japan. This work was partly supported by a Grant-in-Aid for Challenging Research (Pioneering) JP20K20573 to AY; Scientific Research JP20H03054 (B) to AY, JP19H03037 (B) to AY, JP21H02263 (B) to KM, JP17H01483 (A) to AY, and JP17H04715 to DN from the Japanese Society for the Promotion of Science (JSPS); and the Joint Research Program of the Institute of Low Temperature Science, Hokkaido University.

Appendix A. Supplementary material

Supplementary data to this article can be found online at https://doi.org/10.1016/j.pocean.2023.103117.

References

Aoki, S., Yamazaki, K., Hirano, D., Katsumata, K., Shimada, K., Kitade, Y., Sasaki, H., Murase, H., 2020. Reversal of freshening trend of Antarctic Bottom Water in the Australian-Antarctic Basin during 2010s. Sci. Rep. 10, 14415. https://doi.org/10.1038/s41598-020-71290-6.

Armand, L.K., Crosta, X., Romero, O., Pichon, J.-J., 2005. The biogeography of major diatom taxa in Southern Ocean sediments:1. Sea ice related species. Palaeogeogr. Palaeoclimatol. Palaeoecol. 223 (1–2), 93–126. https://doi.org/10.1016/j.palaeo.2005.02.015.

Arrigo, R.K., Thomas, M., Michael, P.L., 2010. Primary producers and sea ice. In: David, N.T., Gerhard, S.D. (Eds.), Sea Ice, 2nd edition. Wiley-Blackwell, Hoboken, NJ, pp. 283–326.

Assmy, P., Henjes, J., Smetacek, V., Montresor, M., 2006. Auxospore formation by the silica-sinking, oceanic diatom Fragilariopsis kerguelensis (Bacillariophyceae). J. Phycol. 42, 1002–1006. https://doi.org/10.1111/j.1529-8817.2006.00260.x.

Biggs, T.E., Alvarez-Fernandez, S., Evans, C., Mojica, K.D.A., Rozema, P.D., Venables, H. J., Pond, D.W., Brussaard, C.P., 2019. Antarctic phytoplankton community composition and size structure: importance of ice type and temperature as regulatory factors. Polar Biol. 42 (11), 1997–2015. https://doi.org/10.1007/s00300-019-02576-3.

Boyd, P.W., Law, C.S., 2001. The Southern Ocean iron release experiment (SOIREE)—introduction and summary. Deep-Sea Res. II 48 (11–12), 2425–2438.

Chiba, S., Hirawake, T., Ushio, S., Horimoto, N., Satoh, R., Nakajima, Y., Ishimaru, T., Yamaguchi, Y., 2000. An overview of the biological/oceanographic survey by the RTV Umitaka-Maru III off Adelie Land, Antarctica in January-February 1996. Deep-Sea Res. II 47 (12–13), 2589–2613. https://doi.org/10.1016/S0967-0645(00)00037-0.

Clarke, D.B., Ackley, S.F., 1984. Sea ice structure and biological activity in the Antarctic marginal ice zone. J. Geophys. Res. Oceans 89, 2087–2095. https://doi.org/10.1029/JC089iC02p02087.

Clementson, L.A., Parslow, J.S., Griffiths, F.B., Lyne, V.D., Mackey, D.J., Harris, G.P., McKenzie, D.C., Bonham, P.I., Rathbone, C.A., Rintoul, S., 1998. Controls on phytoplankton production in the Australasian sector of the subtropical convergence. Deep-Sea Res. I 45, 1627–1661. https://doi.org/10.1016/S0967-0637(98)00035-1.

Cortese, G., Gersonde, R., 2007. Morphometric variability in the diatom *Fragilariopsis kerguelensis*: Implications for Southern Ocean paleoceanography. Earth Planet Sci. Lett. 257, 526–544. https://doi.org/10.1016/j.epsl.2007.03.021.

Crosta, X., 2009. Holocene size variations in two diatom species off East Antarctica: Productivity vs environmental conditions. Deep-Sea Res. I 56, 1983–1993. https://doi.org/10.1016/j.dsr.2009.06.009.

Davidson, A.T., Scott, F.J., Nash, G.V., Wright, S.W., Raymond, B., 2010. Physical and biological control of protistan community composition, distribution and abundance in the seasonal ice zone of the Southern Ocean between 30 and 80°E. Deep-Sea Res. II 57, 828–848. https://doi.org/10.1016/j.dsr2.2009.02.011.

de Baar, H.J.W., Van Leeuwe, M.A., Scharek, R., Goeyens, L., Bakker, K.M.J., Fritsche, P., 1997. Nutrient anomalies in Fragilariopsis kerguelensis blooms, iron deficiency and the nitrate/phosphate ratio (A. C. Redfield) of the Antarctic Ocean. Deep-Sea Res. II 44, 229–260. https://doi.org/10.1016/S0967-0645(96)00102-6.

Deppeler, S.L., Davidson, A.T., 2017. Southern Ocean phytoplankton in a changing climate. Front. Mar. Sci. 4, 40. https://doi.org/10.3389/fmars.2017.00040.

Dieckmann, G.S., Lange, M.A., Ackley, S.F., Jennings Jr., J.C., 1991. The nutrient status in sea ice of the Weddell Sea during winter: effects of sea ice texture and algae. Polar Biol. 11, 449–456. https://doi.org/10.1007/BF00233080.

Dufrêne, M., Legendre, P., 1997. Species assemblages and indicator species: the need for a flexible asymmetrical approach. Ecol. Monogr. 67, 345–366. https://doi.org/10.1890/0012-9615(1997)067[0345:SAAIST]2.0.CO;2.

Edlund, M.B., Stoermer, E.F., 1997. Ecological, evolutionary and systematic significance of diatom life histories. J. Phycol. 33, 897–918. https://doi.org/10.1111/j.0022-3646.1997.00897.x.

El-Sayed, S.Z., Taguchi, S., 1981. Primary production and standing crop of phytoplankton along the ice-edge in the Weddell Sea. Deep-Sea Res. II 28, 1017–1032. https://doi.org/10.1016/0198-0149(81)90015-7.

Field, J.G., Clarke, K.R., Warwick, R.M., 1982. A practical strategy for analyzing multispecies distribution patterns. Mar. Ecol. Prog. Ser. 8, 37–52.

Finkel, Z.V., Beardall, J., Flynn, K.J., Quigg, A., Rees, T.A.V., Raven, J.A., 2010. Phytoplankton in a changing world: cell size and elemental stoichiometry. J. Plankton Res. 32 (1), 119–137. https://doi.org/10.1093/plankt/fbp098.

Fryxell, G.A., Kendrick, G.A., 1988. Austral spring microalgae across the Weddell Sea ice edge: spatial relationships found along a northward transect during AMERIEZ 83. Deep-Sea Res. A 35, 1–20.

Garrison, D.L., Buck, K.R., 1989. The biota of Antarctic pack ice in the Weddell sea and Antarctic Peninsula regions. Polar Biol. 10, 211–219. https://doi.org/10.1007/BF00238497.

Garrison, D.L., Buck, K.R., Fryxell, G.A., 1987. Algal assemblages in Antarctic pack ice and in ice-edge plankton. J. Phycol. 23 (4), 564–572. https://doi.org/10.1111/j.1529-8817.1987.tb04206.x.

Gilmer, R.W., 1972. Free-floating mucus webs: a novel feeding adaptation for the open ocean. Science 176, 1239–1240. https://doi.org/10.1126/science.176.4040.1239.

Gomi, Y., Umeda, H., Fukuchi, M., Taniguchi, A., 2005. Diatom assemblages in the surface water of the Indian Sector of the Antarctic Surface Water in summer of 1999/2000. Polar Biosci. 18, 1–15.

Hasle, G.R., Syvertsen, E.E., 1997. Marine diatoms. In: Tomas, C.R. (Ed.), Identifying Marine Phytoplankton. Academic Press, San Diego, pp. 5–385.

Hegseth, E.N., von Quillfeldt, C.H., 2002. Low phytoplankton biomass and ice algal blooms in the Weddell Sea during the ice-filled summer of 1997. Antarct. Sci. 14, 231–243. https://doi.org/10.1017/S095410200200007X.

Herberich, E., Sikorski, J., Hothorn, T., 2010. A robust procedure for comparing multiple means under heteroscedasticity in unbalanced designs. PLOS ONE 5, e9788.

Hirano, D., Mizobata, K., Sasaki, H., Murase, H., Tamura, T., Aoki, S., 2021. Poleward eddy-induced warm water transport across a shelf break off Totten Ice Shelf, East Antarctica. Commun. Earth Environ. 2, 153. https://doi.org/10.1038/s43247-021-00217-4.

Hosie, G.W., Schultz, M.B., Kitchener, J.A., Cochran, T.G., Richards, K., 2000. Macrozooplankton community structure off East Antarctica (80–150°E) during Austral summer of 1995/1996. Deep-Sea Res. II 47, 2437–2463. https://doi.org/10.1016/S0967-0645(00)00031-X.

Iida, T., Odate, T., 2014. Seasonal variability of phytoplankton biomass and composition in the major water masses of the Indian Ocean sector of the Southern Ocean. Polar Sci. 8, 283–297. https://doi.org/10.1016/j.polar.2014.03.003.

Jacques, G., Fukuchi, M., 1994. Phytoplankton of Indian Antarctic Ocean. In: El-Sayed, S. Z. (Ed.), Southern Ocean Ecology: The BIOMASS perspective. Cambridge University Press, New York, pp. 63–78.

Jacques, G., Panouse, M., 1991. Biomass and composition of size fractionated phytoplankton in the Weddell-Scotia confluence area. Polar Biol. 11, 315–328. https://doi.org/10.1007/BF00239024.

JGOFS., 1994. Protocols for the Joint Global Ocean flux study core measurements. International JGOFS Report Series, vol. 19. Bergen, Norway: JGOFS International Project Office.

Kang, S.H., Fryxell, G.A., 1993. Phytoplankton in the Weddell Sea, Antarctica: composition, abundance and distribution in water-column assemblages of the marginal ice-edge zone during austral autumn. Mar. Biol. 116, 335–348. https://doi.org/10.1007/BF00350024.

Kanna, N., Toyota, T., Nishioka, J., 2014. Iron and macro-nutrient concentrations in sea ice and their impact on the nutritional status of surface waters in the southern Okhotsk Sea. Prog Oceanogr 126, 44–57.

Kloster, M., Kauer, G., Esper, O., Fuchs, N., Beszteri, B., 2018. Morphometry of the diatom *Fragilariopsis kerguelensis* from Southern Ocean sediment: High-throughput measurements show second morphotype occurring during glacials. Mar. Micropaleontol. 143, 70–79. https://doi.org/10.1016/j.marmicro.2018.07.002.

Kopczynska, E.E., 1992. Dominance of microflagellates over diatoms in the Antarctic areas of deep vertical mixing and krill concentrations. J. Plankton Res. 14, 1031–1054. https://doi.org/10.1093/plankt/14.8.1031.

Kopczynska, E.E., Weber, L.H., El-Sayed, S.Z., 1986. Phytoplankton species composition and abundance in the Indian sector of the Antarctic Ocean. Polar Biol. 6, 161–169. https://doi.org/10.1007/BF00274879.

Lafond, A., Leblanc, K., Legras, J., Cornet, V., Quéguiner, B., 2020. The structure of diatom communities constrains biogeochemical properties in surface waters of the Southern Ocean (Kerguelen Plateau). J. Mar. Syst. 212, 103458.

Lannuzel, D., Vancoppenolle, M., de Jong, J., Meiners, K. M., Grotti, M., Nishioka, J., Schoemann, V. 2016. Iron in sea ice: Review and new insights. Element. Sci. Anth. 4, 000130. 10.12952/journal.elementa.000130.

Lizotte, M.P., 2001. The contributions of sea ice algae to Antarctic marine primary production. Am. Zool. 41 (1), 57–73. https://doi.org/10.1093/icb/41.1.57.

Marañón, E., 2015. Cell size as a key determinant of phytoplankton metabolism and community structure. Annu. Rev. Mar. Sci. 7, 241–264. https://doi.org/10.1146/annurev-marine-010814-015955.

Marañón, E., Van Wambeke, F., Uitz, J., Boss, E.S., Dimier, C., Dinasquet, J., Engel, A., Haëntjens, N., Pérez-Lorenzo, M., Taillandier, V., Zäncker, B., 2021. Deep maxima of phytoplankton biomass, primary production and bacterial production in the Mediterranean Sea. Biogeosciences 18 (5), 1749–1767. https://doi.org/10.5194/bg-18-1749-2021.

Marra, J., Boardman, D.C., 1984. Late winter chlorophyll *a* distributions in the Weddell Sea. Mar. Ecol. 9, 197–205.

Martin, J.H., Fitzwater, S.E., Gordon, R.M., 1990. Iron deficiency limits phytoplankton growth in Antarctic waters. Global Biogeochem. Cycles 4, 5–12. https://doi.org/10.1029/GB004i001p00005.

Moline, M.A., Karnovsky, N.J., Brown, Z., Divoky, G.J., Frazer, T.K., Jacoby, C.A., Torres, J.J., Fraser, W.R., 2008. High latitude changes in ice dynamics and their impact on polar marine ecosystems. Ann. N. Y. Acad. Sci. 1134 (1), 267–319. https://doi.org/10.1196/annals.1439.010.

Nicol, S., Pauly, T., Bindo, N.L., Strutton, P.G., 2000. 'BROKE' a biological/oceanographic survey off the coast of East Antarctica (80–150°E) carried out in January-March 1996. Deep-Sea Res. II 47, 2281–2298. https://doi.org/10.1016/S0967-0645(00)00026-6.

Orsi, A.H., Whitworth III, T., Nowlin Jr, W.D., 1995. On the meridional extent and fronts of the Antarctic Circumpolar Current. Deep-Sea Res. I 42 (5), 641–673. https://doi.org/10.1016/0967-0637(95)00021-W.

Pearce, I., Scott, F., 2021. Antarctic Marine Protists | Interactive taxonomic keys, All Factsheets. https://taxonomic.aad.gov.au/599.html, last accessed at 1/20/2021.

Perissinotto, R., 1992. Mesozooplankton size-selectivity and grazing impact on the phytoplankton community of the Prince Edward Archipelago (Southern Ocean). Mar. Ecol. Prog. Ser. 79 (3), 243–258.

Pinkernell, S., Beszteri, B., 2014. Potential effects of climate change on the distribution range of the main silicate sinker of the Southern Ocean. Ecol. Evol. 4 (16), 3147–3161.

Quéguiner, B., 2013. Iron fertilization and the structure of planktonic communities in high nutrient regions of the Southern Ocean. Deep-Sea Res. II 90, 43–54.

Quetin, L.B., Ross, R.M., 1985. Feeding by Antarctic krill, *Euphausia superba*: does size matter? In: Siegfried, W.R., Condy, P.R., Laws, R.M. (Eds.), Antarctic nutrient cycles and food webs. Springer, Berlin, pp. 372–377.

Quinn, G.P., Keough, M.J., 2002. Experimental Design and Data Analysis for Biologists. Cambridge University Press, New York.

R Core Team, 2021. R: A language and environment for statistical computing. R Foundation for Statistical Computing, Vienna, Austria https://www.R-project.org/.

Ragueneau, O., Schultes, S., Bidle, K., Claquin, P., Moriceau, B., 2006. Si and C interactions in the world ocean: Importance of ecological processes and implications

for the role of diatoms in the biological pump. Global Biogeochem. Cycles 20 (4), GB4S02. https://doi.org/10.1029/2006GB002688.
Sallée, J.-B., Speer, K.G., Rintoul, S.R., 2010. Zonally asymmetric response of the Southern Ocean mixed-layer depth to the Southern Annular Mode. Nat. Geosci. 3, 273–279. https://doi.org/10.1038/ngeo812.
Samyshev, E.Z., 1991. Antarctic krill and the structure of planktonic community in its distribution area. "Nauka" Publishing, Moscow.
Sedwick, P.N., DiTullio, G.R., 1997. Regulation of algal blooms in Antarctic shelf waters by the release of iron from melting sea ice. Geophys. Res. Lett. 24 (20), 2515–2518. https://doi.org/10.1029/97GL02596.
Shannon, C.E., Weaver, W., 1949. The mathematical theory of communication. The University of Illinois Press, Urbana.
Shukla, S.K., Crosta, X., Cortese, G., Nayak, G.N., 2013. Climate mediated size variability of diatom *Fragilariopsis kerguelensis* in the Southern Ocean. Quat. Sci. Rev. 69, 49–58. https://doi.org/10.1016/j.quascirev.2013.03.005.
Smetacek, V.S., 1985. Role of sinking in diatom life-history cycles: ecological, evolutionary and geological significance. Mar. Biol. 84 (3), 239–251.
Smith, W.O., Nelson, D.M., 1985. Phytoplankton bloom produced by a receding ice edge in the Ross Sea: Spatial coherence with the density field. Science 227, 163–166. https://doi.org/10.1126/science.227.4683.163.
Sokolov, S., Rintoul, S.R., 2009. Circumpolar structure and distribution of the Antarctic Circumpolar Current fronts: 2. Variability and relationship to sea surface height. J. Geophys. Res. 114, C11019. https://doi.org/10.1029/2008JC005248.
Strutton, P.G., Griffiths, F.B., Waters, R.L., Wright, S.W., Bindoff, N.L., 2000. Primary productivity off the coast of East Antarctica (80–150°E): January to March 1996. Deep-Sea Res. II 47, 2327–2362. https://doi.org/10.1016/S0967-0645(00)00028-X.
Sukhanova, I.N., 1978. 5.2.2 Settling without the inverted microscope. In: Sournia, A. (Ed.), Phytoplankton manual. United Nations Educational, Scientific and Cultural Organization, Paris, pp. 97.
Tilzer, M.M., Dubinsky, Z., 1987. Effects of temperature and day length on the mass balance of Antarctic phytoplankton. Polar Biol. 7, 35–42.
Timmermans, K.R., van der Wagt, B., 2010. Variability in cell size, nutrient depletion, and growth rates of the Southern Ocean diatom Fragilariopsis kerguelensis (Bacillariophyceae) after prolonged iron limitation. J. Phycol. 46 (3), 497–506. https://doi.org/10.1111/j.1529-8817.2010.00827.x.
Tozawa, M., Nomura, D., Nakaoka, S., Kiuchi, M., Yamazaki, K., Hirano, D., Aoki, S., Sasaki, H., Murase, H., 2022. Seasonal variations and drivers of surface ocean pCO_2 in the seasonal ice zone of the eastern Indian sector, Southern Ocean. J. Geophys. Res. 127 https://doi.org/10.1029/2021JC017953.
Urabe, I., Matsuno, K. Sugioka, R., Driscoll, R., Schaafsma, F.L., Yamaguchi, A., Matsukura, R., Sasaki, H., Murase, H. Spatio-temporal changes in the macrozooplankton community in the eastern Indian sector of the Southern Ocean during austral summer: comparison between 1996 and 2018/2019. Prog. Oceanogr. this special issue.
Waters, R.L., van den Enden, R., Marchant, H.J., 2000. Summer microbial ecology off East Antarctica (80–150°E): Protistan community structure and bacterial abundance. Deep-Sea Res. II 47, 2401–2435. https://doi.org/10.1016/S0967-0645(00)00030-8.
Wright, S.W., van den Enden, R.L., 2000. Phytoplankton community structure and stocks in the East Antarctic marginal ice zone (BROKE survey, January-March 1996) determined by CHEMTAX analysis of HPLC pigment signatures. Deep-Sea Res. II 47, 2363–2400. https://doi.org/10.1016/S0967-0645(00)00029-1.
Yamazaki, K., Aoki, S., Shimada, K., Kobayashi, T., Kitade, Y., 2020. Structure of the subpolar gyre in the Australian-Antarctic Basin derived from Argo Floats. J. Geophys. Res. Oceans 125. https://doi.org/10.1029/2019JC015406.
Yamazaki, K., Aoki, S., Katsumata, K., Hirano, D., Nakayama, Y., 2021. Multidecadal poleward shift of the southern boundary of the Antarctic Circumpolar Current off East Antarctica. Sci. Adv. 7 (24), eabf8755. https://doi.org/10.1126/sciadv.abf8755.
Zielinski, U., Gersonde, R., 1997. Diatom distribution in Southern Ocean surface sediments (Atlantic sector): Implications for paleoenvironmental reconstructions. Palaeogeogr. Palaeoclimatol. Palaeoecol. 129 (3–4), 213–250. https://doi.org/10.1016/S0031-0182(96)00130-7.
Zuur, A.F., Ieno, E.N., Walker, N.J., Saveliev, A.A., Smith, G.M., 2009. Mixed effects models and extensions in ecology with R. Springer, New York.